FATIGUE BEHAVIOUR OF DENTAL CERAMICS BASED ON ZrO_2-Al_2O_3 COMPOSITES [1]

Renato Chaves Souza [2]
Claudinei dos Santos[3]
Miguel R. J. Barboza [4]
Luis A. Bicalho [5]
Kurt Strecker [6]
Carlos A. R. P. Baptista [7]

Abstract
The objective of this work was to evaluate the cyclic fatigue strength of commercial pre-sintered Alumina-zirconia composite ceramics for CAD/CAM systems. Samples were sintered in air at 1600°C for 120 minutes with heating and cooling rates of 10^0C/min. The sintered specimens were characterized by X-Ray diffraction and scanning electron microscopy. The cyclic fatigue tests were realized as four-point bending (470 – 530MPa) tests within a frequency of 25 Hz and a stress ratio R of 0.1. The Weibull analysis was employed in order to perform failure probability calculations. The fatigue tests results allow concluding that the fatigue strength limit over 5 x 10^6 stress cycles is about 430MPa or around 63% of the static strength of this material. The fatigue strength limit around 430 MPa is interesting for application in dental implant parts.
Key words: Dental ceramic; Sintering; Mechanical properties; Fatigue; Characterization.

RESPOSTA EM FADIGA DE CERÂMICAS DENTARIAS A BASE DO COMPÓSITO ZrO_2-Al_2O_3

Resumo
O objetivo deste trabalho foi estudar o comportamento em fadiga de compósitos cerâmicos a base de ZrO_2-Al_2O_3 utilizados como material dentário. Blocos pré-sinterizados compostos de 80% de ZrO_2-Y_2O_3 e 20% de Al_2O_3 foram sinterizados a 1600^0C, sendo sem seguida cortados (3x4x45mm), retificados, lixados e polidos. Os CPs foram submetidos a ensaios de fadiga por flexão em 4 pontos, em diferentes tensões operada sob controle de carga, com uma forma de onda senoidal em uma freqüência de 25Hz e razão de tensão R=0,1 até a fratura ou aproximadamente de 2 a 5 x 10^6 ciclos. Curvas de fadiga foram obtidas, superfícies de fratura foram submetidas a MEV e difração de raios-X. Os resultados indicam um limite de resistência a fadiga em tensões próximas a 430MPa, valores muito superiores aos limites de tensão proporcionais a cargas mastigatórias geradas em seres humanos., o que viabiliza o seu uso como materiais para próteses dentarias.
Palavras-chave: Biomateriais; Caracterizações; Fadiga.

[1] *Technical contribution to 64th ABM Annual Congress, July, 13th to 17th, 2009, Belo Horizonte, MG, Brazil.*
[2] *Professor - Escola Técnica Federal - CEFET-SP*
[3] *Professor - Faculdade de Tecnologia – UERJ-FAT*
[4] *Professor - Escola de Engenharia de Lorena - Universidade de São Paulo - EEL-USP*
[5] *Doctoral student - Escola de Engenharia de Lorena - Universidade de São Paulo - EEL-USP*
[6] *Professor - Universidade Federal de São João Del'Rei - UFSJ*
[7] *Professor - Escola de Engenharia de Lorena - Universidade de São Paulo - EEL-USP*

1 INTRODUCTION

Ceramic components for structural engineering applications are generally subjected to continuous operation in a variable load environment.[1] Usually, ceramics are characterized in regard to hardness, toughness and bending strength. However, the failure under fatigue conditions, at loads much below the critical failure strength is a common phenomenon in all materials, including ceramics.[2] Consequently, it is very important to investigate the fatigue strength of ceramics.

The development of advanced ceramics during recent years followed several fascinating concepts, e. g., to increase strength, reduce brittleness, and increase high temperature stability. However, the development of structural ceramics with improved fatigue resistance was not considered. The existence of cyclic fatigue effects has been proven for several ceramic materials, and clear experimental evidence has been obtained for a limited range of test conditions.[3]

Another possibility of application for ceramic materials is as biomaterials. In this case, the use of advanced ceramics started in the 1970'ies, and since then a continuous improvement of these materials in various applications can be noted. An important improvement has been possible by the use of ceramics as dental materials. They present advantages such as aesthetic, biocompatibility and chemical inertness.[4-6]

Zirconia is the most promising bio-ceramic, due to its excellent biocompatibility. The main advantages of ZrO_2 are its higher fracture strength and fracture toughness, and lower Young's modulus.[7-13] On the other hand, Alumina ceramics enable improvements of hardness and wear resistance on the composite ceramics based on zirconia matrix. It is of common knowledge that ZrO_2 additions may increase the fracture toughness of ceramic materials. This effect is based on the tetragonal to monoclinic (t-m) phase transformation of ZrO_2, accompanied by an increase of the specific volume in the order of 3-6%.[7] This volume increase generates stresses in the ceramic matrix, which difficult crack propagation. When such a ceramic is used for implants such as artificial joints or dental abutment, it undergoes cyclic loading for a fairly long period.[14]

Cyclic fatigue of ceramics recently became a highly attractive research field for material scientists. There is a strong demand to generate design-relevant fatigue data which are required for many of the projected applications of structural ceramics. On the other hand, knowledge of fatigue in ceramics is insufficient so far and information about the correlation between microstructural parameters and fatigue properties is still missing for most ceramic systems. Besides this lack of understanding a number of fundamental questions still have not been answered unambiguously for many of the most important ceramics.[15-18]

It is essential in engineering applications of ceramic materials for structural purposes to determine the fatigue behavior under appropriated static or cyclic loading. A considerable number of reports have been published on the fatigue of glass, alumina and zirconia ceramics. There have been few critical studies published regarding the cyclic and static fatigue at room temperature of advanced ceramics, although activity in this field has increased recently. Furthermore, fatigue testing applied to brittle materials imposes a number of problems. One of them is the wide scatter in data, which sometimes obscures the fatigue tendency. This scatter is considered to derive intrinsically from a defect distribution in the specimens.[19]

This research is focused on the processing, mechanical properties and cyclic fatigue life of a commercial Y_2O_3 stabilized ZrO_2–Al_2O_3 composite ceramic.

Specifically, the fatigue behavior of tetragonal zirconia polycrystals (TZP) with 3mol% of Y_2O_3 doped with 20wt.% of Al_2O_3, produced by solid-state sintering at 1600°C was investigated by means of cyclic four-point bending load controlled tests. The occurrence of t-m transformation during the fatigue tests was observed.

2 EXPERIMENTAL PROCEDURE

2.1 Processing

High-purity ZrO_2(3%Y_2O_3)-20wt.%Al_2O_3 composite pre-sintered blocks (ProtMat Materiais Avançados®-Brazil) were used in this study. Blocks with 55x15x15mm were cut and sintered at 1.600°C in a $MoSi_2$ resistance furnace heated for 2h, with heating and cooling rates of 10°C/min.[5,11,12]
In order to obtain the specimens for the four-point flexure tests, the dense ceramic blocks were cut and grinded in rectangular bars of 3 x 4 x 45 mm, with an automatic grinding machine. After grinding, the samples were polished with diamond pastes of 15 μm, 9 μm, 6 μm, 3 μm and 1 μm.

2.2 Characterization

The bulk density of the sintered samples was measured by the Archimedes' method in distilled water. The crystalline phase content was determined by X-ray diffractometry (XRD) using Cu-kα radiation in the 2θ range of 20° to 80°, with a step width of 0.05° and 2s of exposure time per position. The monoclinic phase fraction was calculated using the Garvie and Nicholson[20] method and the monoclinic volume fraction was then obtained using the equation proposed by Toraya *et al.*[21] The calculation of the penetration depth of the X-rays of the analyzed surface was based on the absorption of the X-rays by the material. The penetration depth of X-rays is given by Eq. (1):[22]

$$h = -\frac{sen\,\theta}{2.\frac{\mu}{\rho}\rho}\left[\ln\frac{I}{I_0}\right] \tag{1}$$

with

$$\frac{\mu}{\rho} = w_1\left(\frac{\mu}{\rho}\right)_1 + w_2\left(\frac{\mu}{\rho}\right)_2 + \ldots \tag{2}$$

Where:
h = penetration depth [μm]; θ = diffraction angle, I = intensity of diffracted X-ray beam, I_0 = intensity of X-ray beam, μ = coefficient of absorption; w = weight fraction of element or component; μ/ρ = coefficient of mass absorption [cm^2/g] (Zr = 143, O = 11.5, Y = 134); ρ = specific mass [g/cm^3] (Zr = 6.511, O = 1.354, Y = 4.472, ZrO_2.3%Y_2O_3 = 6.051).

Polished and thermal etched surfaces of the sintered samples and fractured surfaces of the mechanically tested specimens, were examined by scanning electron microscopy (SEM), using a LEO-1450VP microscope.

2.3 Microhardness and Fracture Toughness

Hardness and fracture toughness, K_{IC}, were determined using the Vickers Indentation method. In each sample, 21 indentations were measured, under a load of

2000 gf for 30 s. The fracture toughness was calculated by measurement of the relation between crack length (*c*) and indentation length (*a*), using the relation proposed by Niihara et al.,[23] valid for Palmqvist crack types, which present *c*/*a* <3.5.

2.4 Modulus of Rupture (MOR)

The modulus of rupture (MOR) was determined by four-point bending tests, using a servo-hydraulic testing machine MTS model 810.23M. For the accomplishment of the bending tests, batches of 21 samples were grinded and polished, obtaining bars of 4 x 3 x 45 mm, according ASTM C 1116 - 94. The tests were conducted using a four-point bending device with outer and inner spans (I_1 and I_2) of 40 mm and 20 mm respectively. The speed of the crosshead displacement was 0.5 mm/min. The bending strength of the samples was calculated by Eq. (3).

$$\sigma_f = \frac{3}{2} F_A \times \frac{(I_1 - I_2)}{b \times h^2} \tag{3}$$

Where: σ_f = Bending strength [MPa]; F_A = Rupture load [N]; b = Width of the samples [mm] ; h = Height of the samples [mm] ; I_1 = Outer span [mm] ; I_2 = Inner span [mm]

2.5 Cyclic Fatigue

The cyclic fatigue tests were carried out by four-point bending loading in air at room temperature, with a relative humidity near 60%. The specimen dimensions and the testing machine were the same as employed in the bending strength tests. The cyclic fatigue was studied under a sinusoidal stress wave form with a frequency of 25Hz and a constant stress ratio (R) between the minimum stress (σ_{min}) and maximum stress (σ_{max}) of 0.1. The number of specimens used in fatigue tests varied between 10 and 20 samples at each stress level, under the maximum stress values of 470 MPa, 500 Mpa and 530 MPa. The tests were interrupted when the surviving samples reached a number of stress cycles between 2 and 5 x 10^6 cycles. Interrupted samples were submitted to XRD and SEM characterization according to procedures previously mentioned.

2.6 Statistical Analysis

For the statistical evaluation of the fracture strength, the two-parameter Weibull distribution function, given by Eq. (4), was used.

$$P(x) = 1 - \exp\left(-\left(\frac{x}{b}\right)^m\right) \qquad \text{for } x > 0 \text{ and} \tag{4}$$

$$P(x) = 0 \qquad \text{for } x \leq 0 \quad .$$

Where: P = probability associated to x value (or Failure probability), m =modulus of Weibull distribution, b = scale parameter or characteristic strength, x = bending strength (static tests) or the number of cycles to failure (fatigue tests)
The Weibull parameters, *m* and *b*, are obtained by the linearization of Eq. (4), see Eq. (5)**,** and plotting *ln ln* [1/(1-P(*x*))] vs *ln* $\tilde{x}$

$$\ln\ln\left(\frac{1}{1 - P(x)}\right) = m\ln(x) - m\ln(b) \tag{5}$$

The stress value for 50% of rupture probability was estimated as reference and also for direct comparison with the average fracture strength. The Weibull parameter "*m*" for the static tests, was determined using a correction factor of 0.938, corresponding to 21 samples, in agreement with the German norm DIN-51-110.[24]

3 RESULTS AND DISCUSSION

3.1 Characterization

Figure 1 presents X-ray diffractogram (XRD) patterns of the ZrO_2-Al_2O_3 samples after sintering at 1.600°C.

It can be observed that sintered ceramic presents only tetragonal zirconia and alumina phases. No considerable amounts of residual monoclinic ZrO_2 phase, which was estimated according to Toraya *et al.,*[21] was observed on the sintered samples. In this case the application of stresses to tetragonal ZrO_2 grains may start the martensitic *t-m* transformation[5] improving the bending strength of these ceramics.

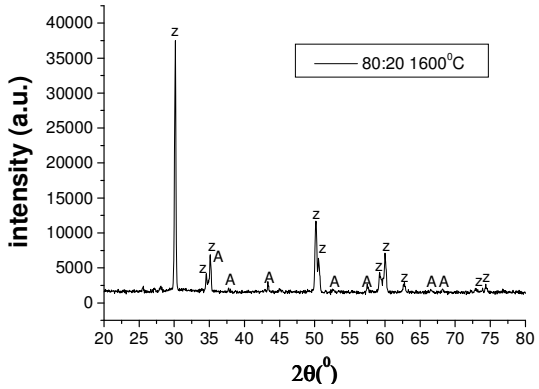

Figure 1. X-ray diffractogram patterns of the zirconia alumina composites. (Z – Tetragonal ZrO_2; A – Al_2O_3).

Figure 2 presents a micrograph of the polished and etched ZrO_2-Al_2O_3 surface and the fracture surface of a specimen tested in fatigue.

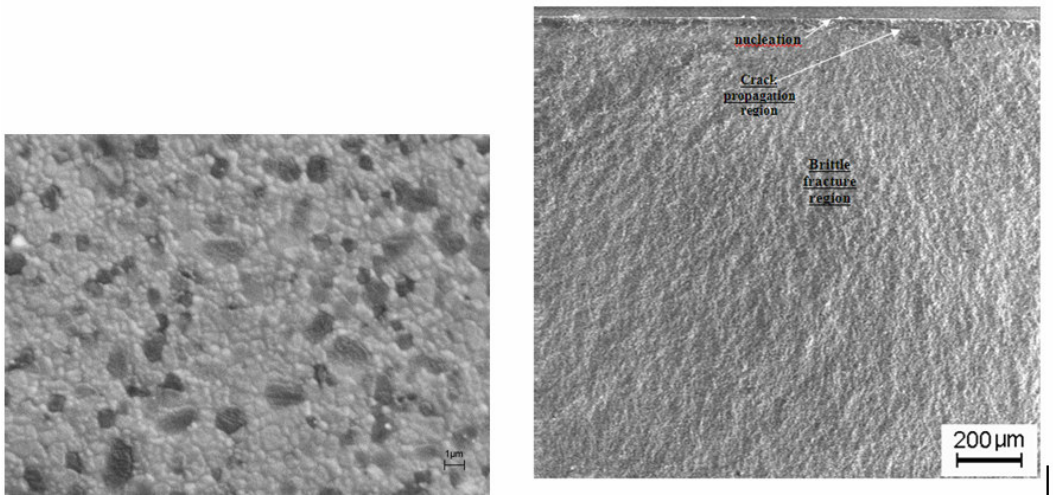

(a) (b)

Figure 2. Micrograph of the ZrO_2 – Al_2O_3 samples: a) polished surface, b) fracture surface.

Looking at a typical microstructure of the sintered samples (Figure 2(a)), the presence of fine microstructure composed of equiaxial grains smaller than 0.5μm can be observed. No abnormal grain growth of ZrO_2 grains was observed in this material. In Figure 2(b) a typical brittle fracture surface which clearly shows that the initial crack nucleation and propagation region are located in the upper side of the picture, corresponding to the region of maximum tensile stress in the bending test.

3.2 Microhardness, Fracture Toughness and Modulus of Rupture (MOR)

Table 1 presents the relative density and mechanical properties of the sintered samples.

Table 1 Properties of the sintered samples.

Relative Density (%)	Vickers Hardness (HVn)	Fracture Toughness ($MPam^{1/2}$)	MOR (MPa)	Weibull modulus
99.8±0.2	1520±15	8.0± 0.2	680±35	11.7

The high densification (> 99.5%) of the sintered samples, indicates that the sintering conditions used in this work were satisfactory to eliminate most of the porosity and maintain a microstructure with fine grains, see Figure 2(a). This typical microstructure and the results of the X-ray diffraction analysis, shown in Figure 1(b), indicate the predominance of the tetragonal phase, justifying the high K_{IC} and MOR values presented in Table 1. Toughening by the *t-m phase transformation and crack deflection* are the main mechanisms actuating to improve the mechanical properties of this material.[25] The *t-m* phase transformation, allows the MOR to reach the elevated values, near 700MPa. Furthermore, the hardness values were about 1520 HV. In general, the results obtained in this work are typical and consistent with literature data.[8]

3.3 Cyclic Fatigue

The results of the cyclic fatigue tests are shown in Figure 3 in terms of the stress-life curve which correlates the maximum bending stress level (σ_{max}) to the number of cycles to failure (N_f).

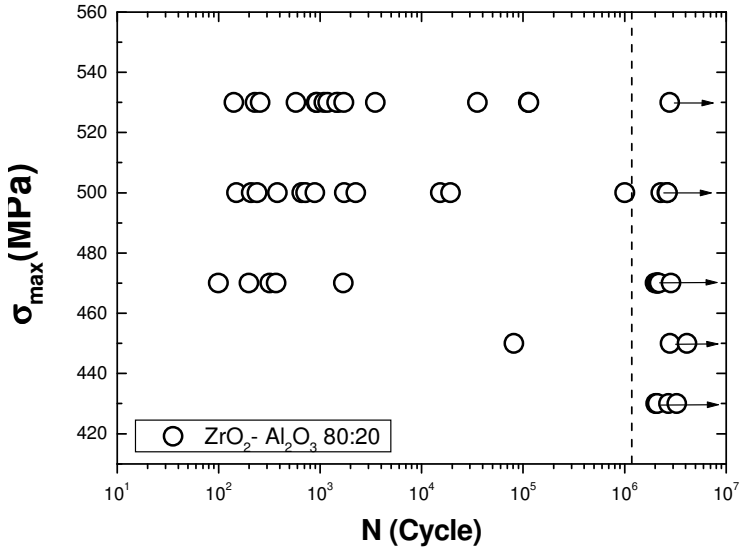

Figure 3. Cyclic fatigue test results of the ZrO_2–Al_2O_3 samples: σ_{max} x N curves.

The cyclic fatigue tests were interrupted at N_f = 2 to 5 x 10^6 cycles, if failure didn't occur. The specimens which did not fracture in the test are marked by an arrow symbol (run out). The five maximum stress levels (σ_{max}) were selected in relation to the initial strength. It was found that the fatigue strength limit is around 430 MPa, which corresponds to 62.5% of the MOR.

At the lowest stress levels (σ_{max} = 430 MPa), neither spontaneous nor fatigue fracture were observed. As σ_{max} increased, some specimens reached N_f = 2 x 10^6 cycles without failure, but some specimens failed spontaneously, i. e., below 10^3 loading cycles. On the other hand, the number of specimens failing at $10^3 < N_f < 2$ x 10^6 was relatively large. In an amount of 9 specimens tested at σ_{max} = 470 MPa, 6 specimens failed below a hundred cycles, 9 failed during cycling and none of them achieved 10^6 cycles.

Thus, samples that failed under low cycles ($N_f < 10^3$ cycles), are more frequent under higher stresses, while the reduction of the maximum applied stress lead to a significant increase in the number of un-failed samples ($N_f > 2$ x 10^6 cycles).

XRD patterns of the polished surfaces submitted to tensile stress, in survived samples after fatigue testing, indicates a low content of the martensitic transformation, during fatigue tests. The penetration depth of X-rays of the analyzed surface, based on the absorption of the X-rays by the material and calculated by Eq. (1) was of 7.3 μm. This penetration depth of X-rays allowed detecting the *t-m* phase transformation in the central region of the polished surface which was submitted to the maximum tensile stress during the bending fatigue tests. The volume fraction of the transformed phase was estimated around 7 to 10%. However the crack shielding presented by the martensitic ZrO_2 $^{(t-m)}$ transformation produces compressive stresses that cause crack arrest.

The Figure 4 presents the fracture surfaces micrographs of sintered samples fractured during fatigue tests.

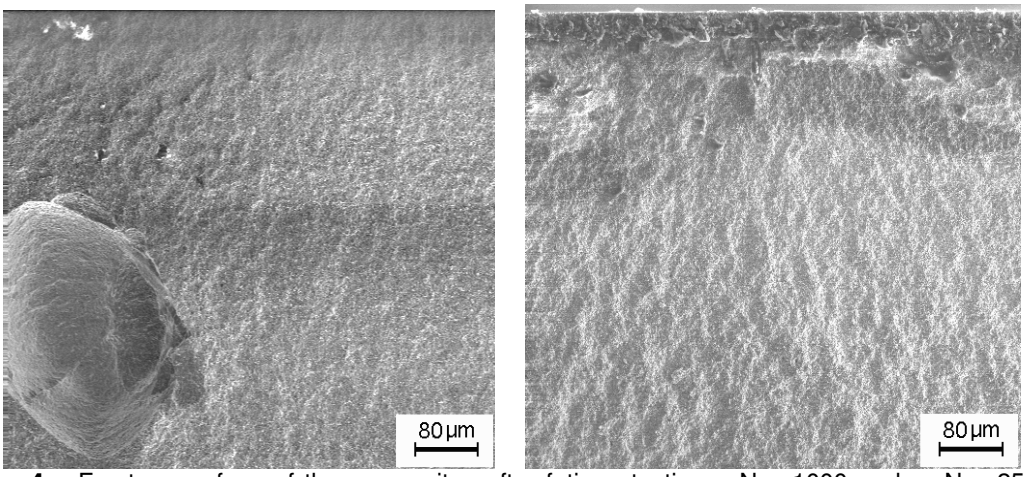

Figure 4 – Fracture surface of the composites after fatigue testing = N = 1000 cycles; N = 250000 cycles.

In these specimens, fatigue fracture start in the polished tensile surface of the sample and occur in a brittle mode, being a function of the critical flaw size. This flaw must overcome the compression stresses generated by the t-m phase transformation in order to propagate. Therefore, the *t-m* transformation as observed by Grathwohl and Liu[15] increases the critical flaw size and results in improved strength and fatigue resistance. Cyclic testing of Y-TZP provides interesting results concerning fatigue behavior, threshold phenomena, and the strengthening effect of this transformation-toughened ceramic. The range of fatigue is not clearly delimited while it is clear that this fine-grained ceramic is particularly prone to cyclic fatigue.

4 CONCLUSIONS

In this work, the mechanical properties and cyclic fatigue behavior of zirconia-alumina composites has been evaluated. The adopted processing route allowed to obtain highly dense (99.8%) materials. The modulus of rupture (680 MPa), Vickers hardness (1520 HV) and fracture toughness (8 $MPa.m^{1/2}$), as well as the Weibull modulus (11.7) qualifies this material for applications in metal-free dental restorations.

Cyclic fatigue tests by four-point bending were conducted in order to obtain the stress life (σ x N) curve for the material. The experimental results indicate that 3Y-TZP-Al_2O_3 ceramic material suffered cyclic fatigue fracture. Phase analysis results indicate that the material suffers t-m phase transformation due to cyclic as well as static loading. It was found that the fatigue strength limit is around 430 MPa (62.5% of the MOR).

Acknowledgements

The authors acknowledge to the *FAPESP* for financial support, under Grants n°. 04/04386-1 and 05/52971-3.

REFERENCES

1 Yao F, Ando K, Chu MC and Sato S. Static and cyclic fatigue behaviour of crack-healed Si3N4/SiC composite ceramics. J Eur Ceram Soc, 2001; 21; 991-997.

2 Basu D and Sarkar BK. Effect of zirconia addition on the fatigue behaviour of fine grained alumina. Bull Mater Scienc, 1992; 24; 101-104.
3 Grathwohl G and Liu T. Strengthening of zirconia-alumina during cyclic fatigue testing. J Amer Ceram Soc, 1989; 72 (10); 1988-1990.
4 Hench LL. Bioceramics. J Amer Ceram Soc, 1998; 81 (7); 1705-1728.
5 Willians DF. Medical and dental materials. VCH Weinheim, New York, 1992.
6 Hench LL and Wilson J. An introduction to bioceramic. Advanced Series in Ceramics, World Scientific, Singapura, 1993; 1; 1-23.
7 De Aza AH, Chevalier J, Fantozzi G, Schehl M and Torrecillas R. Crack growth resistance of alumina, zirconia and zirconia toughened alumina ceramics for joint prostheses. Biomaterials, 2002; 23; 937-945.
8 Stevens R. An introduction to zirconia: zirconia and zirconia ceramics. 2nd ed., Magnesium electrum, Twickenham (Magnesium Elektron Publications, 1986; n113).
9 Basu D and Sarkar BK. Toughness determination of zirconia toughened alumina ceramics from growth of indentation-induced cracks. J Mater Research, 1996; 11 (12); 3057-3062.
10 Basu B, Vleugels J and Van Der Biest O. ZrO_2-Al_2O_3 Composites with tailored toughness. J Alloys and Comp, 2004; 372 (1-2); 278-284.
11 Piconi C and Maccauro G. Zirconia as a ceramic biomaterial. Biomaterials, 1999; 20 (1); 1-25.
12 Piconi C, Burger W, Richter HG, Cittadini A, Maccauro G, Covacci V, Bruzzese N, Ricci GA and Marmo E. Y-TZP ceramics for artificial joint replacements. Biomaterials, 1998; 19 (16); 1489-1494.
13 Stevens R. Zirconia: second phase particle transformation toughening of ceramics. Transac Brit Ceram, 1981; 80; 81-85.
14 Zhu P, Lin Z, Chen G and Kiyohiko I. The predictions and applications of fatigue lifetime in alumina and zirconia ceramics. Int J Fatigue, 2004; 26; 1109-1114.
15 Grathwohl G and Liu T. Crack resistance and fatigue of transforming ceramics: I, materials in the ZrO_2-Y_2O_3-Al_2O_3 system. J Amer Ceram Soc, 1991; 74 (2); 318-325.
16 Grathwohl G and Liu T. Crack resistance and fatigue of transforming ceramics: II, CeO_2-stabilized tetragonal ZrO_2. J Amer Ceram Soc, 1991;74 (12); 3028-3034.
17 Matsuzawa M, Fujimagari E and Horibe S. Cyclic deformation and crack growth in zirconia ceramics. Mat Sci Eng A, 2001; 314 (1-2); 105-109.
18 Matsuzawa M and Horibe S. Resistance against crack nucleation and propagation in Y_2O_3 doped tetragonal zirconia ceramics. Mat Sci Eng A, 2002; 333 (1-2); 199-207.
19 Kawakubo T and Komeya K. Static and cyclic fatigue behavior of a sintered silicon nitride at room temperature. J Amer Ceram Soc, 1987; 70 (6); 400-405.
20 Garvie RC and Nicholson PS. Phase analysis in zirconia systems. J Amer Ceram Soc, 1972; 55; 303-305.
21 Toraya H, Yoshimura M and Somiya S. Calibration curve for quantitative analysis of the monoclinic tetragonal ZrO_2 system by X-ray diffraction. J Amer Ceram Soc, 1984; 67; 119-121.
22 Klug HP and Alexander LE. X-ray diffraction procedures for polycrystalline and amorphous materials. John Wiley and Sons, New York, 1974.
23 Niihara K, Moreno R and Hasselman DPH. J. Mater. Sci. Lett, 1982; 1; 13–16.
24 Lipson C and Sheth NJ. Statistical design and analysis of engineering experiments, McGraw-Hill, New York, 518p, 1973.
25 Fett T. and Munz D. Influence of time-dependent phase transformations on bending tests. Mater Sci and Eng A, 1996; 219; 89-94.
26 Quinn GD. Strenght and proff testing. Engineered Materials Handbook, Vol. 4, Ceramics and Glasses. ASM International, Metals Park, OH, 1991; 585-598.